Available online at www.sciencedirect.com
SCIENCE DIRECT®
Biochemical Pharmacology 65 (2003) 857–875
Biochemical Pharmacology
www.elsevier.com/locate/biochempharm

Toxicogenomics of bromobenzene hepatotoxicity: a combined transcriptomics and proteomics approach

Wilbert H.M. Heijne[a,*], Rob H. Stierum[a], Monique Slijper[b], Peter J. van Bladeren[c], Ben van Ommen[a]

[a]*TNO Nutrition and Food Research, P.O. Box 360, 3700 AJ Zeist, The Netherlands*
[b]*Department of Biomolecular Mass Spectrometry, Utrecht University, Utrecht, The Netherlands*
[c]*Department of Toxicology, Wageningen University and Research Centre, Wageningen, The Netherlands*

Received 23 July 2002; accepted 24 November 2002

Abstract

Toxicogenomics is a novel approach integrating the expression analysis of thousands of genes (transcriptomics) or proteins (proteomics) with classical methods in toxicology. Effects at the molecular level are related to pathophysiological changes of the organisms, enabling detailed comparison of mechanisms and early detection and prediction of toxicity. This report addresses the value of the combined use of transcriptomics and proteomics technologies in toxicology. Acute hepatotoxicity was induced in rats by bromobenzene administration resulting in depleted glutathione levels and reduced average body weights, 24 hr after dosage. These physiological symptoms coincided with many changes of hepatic mRNA and protein content. Gene induction confirmed involvement of glutathione-*S*-transferase isozymes and epoxide hydrolase in bromobenzene metabolism and identified many genes possibly relevant in bromobenzene toxicity. Observed glutathione depletion coincided with induction of the key enzyme in glutathione biosynthesis, γ-glutamylcysteine synthetase. Oxidative stress was apparent from strong upregulation of heme oxygenase, peroxiredoxin 1 and other genes. Bromobenzene-induced protein degradation was suggested from two-dimensional gel electrophoresis, upregulated mRNA levels for proteasome subunits and lysosomal cathepsin L, whereas also genes were upregulated with a role in protein synthesis. Both protein and gene expression profiles from treated rats were clearly distinct from controls as shown by principal component analysis, and several proteins found to significantly change upon bromobenzene treatment were identified by mass spectrometry. A modest overlap in results from proteomics and transcriptomics was found. This work indicates that transcriptomics and proteomics technologies are complementary to each other and provide new possibilities in molecular toxicology.

Keywords: Toxicogenomics; Bromobenzene; cDNA microarray; Transcriptomics; Proteomics; Hepatotoxicity

1. Introduction

Toxicology aims to detect adverse effects of a compound on an organism based on observed symptoms or toxicity markers. However, a wide variety of mechanisms underlie the different types of toxicity at the cellular level. To discriminate between these various types of toxicity, an extension of the methods and markers currently used in toxicology is required. Technologies based on the progression in functional genomics research enable the determination of the expression of thousands of genes (transcriptomics) or proteins (proteomics) in a single experiment. In the novel research discipline toxicogenomics, functional genomics technologies are integrated with classical methods to study toxicity at the molecular level in relation to the pathophysiological changes of the organism. This holistic approach enables detailed comparison of mechanisms and early detection and prediction of toxicity. Primary effects of toxicants on gene expression are triggered upon binding to receptors, whereas secondary effects on gene expression are to be expected as a result of changes in various cellular processes.

* Corresponding author. Tel.: +31-30-694-4137; fax: +31-30-696-0264.
E-mail address: heijne@voeding.tno.nl (W.H.M. Heijne).

Abbreviations: γ-GCS, γ-glutamylcysteine synthetase; APR, acute phase response; BB, bromobenzene; CCl_4, carbon tetrachloride; CDNB, (1-chloro-2,4-dinitrobenzene); CO, corn oil; ESI-MS-MS, electrospray ionisation tandem mass spectrometry; GSH, reduced glutathione; GSSG, oxidised glutathione; GST, glutathione-*S*-transferase; HO-1, heme oxygenase; i.p., intraperitoneal; MALDI-TOF, matrix assisted laser desorption ionisation-time of flight; mRNA, messenger RNA; MS, mass spectrometry; PCA, principal component analysis; UT, untreated.

0006-2952/02/$ – see front matter
doi:10.1016/S0006-2952(02)01613-1

cDNA-microarray based multiple gene expression measurement (transcriptomics) was shown to be a powerful tool in the mechanistic assessment of toxic responses [1–5]. The determination of thousands of gene expression levels simultaneously in a given sample provides an insight in the molecular processes that together determine the specific status of that sample. Gene expression profiles can be used to discriminate samples exposed to different classes of toxicants, to predict toxicity of (yet) unknown compounds and to study cellular mechanisms that lead to or result from toxicity. In analogy to this, the simultaneous measurement of the thousands of proteins in a cell will be of great benefit for toxicology, or even of more importance, while the proteins predominantly act in the cellular reactions rather than the gene transcripts. As all proteins have different properties (mass, isoelectric point, solubility, stability, etc.), the accurate measurement of thousands of proteins in a sample is a very complicated task. In this respect, the great advantage of measuring transcripts is that only one type of biomolecule, the mRNA (with all its different sequences), has to be extracted and quantified. Whether all cellular mechanisms can be identified at the mRNA level is still uncertain. For instance, the process of apoptosis is primarily executed through proteolytic (self)-activation of the caspase cascade. Especially cell-protective responses might be orchestrated through fast modification or subcellular redistribution of proteins already present in the cell. Proteomics technologies may have a better chance to visualise processes that do not involve active biosynthesis, or at least they will be complementary to gene expression analysis. Although relationships between single gene expression and corresponding protein levels have been widely studied, to this date, not much has been published on the relation between large scale transcriptomics and proteomics assessments. Scarce examples are provided in literature, for instance describing changes in *Bacillus subtilis* [6,7]. Ruepp *et al.* [8] describe gene and protein expression in rat liver after acetaminophen (paracetamol) administration, and identified several proteins that changed in acetaminophen hepatotoxicity. It is important to realise that the relationship between mRNA and protein content is heavily dependent on time, cellular localisation as well as stability of the molecules. Transcription of DNA into mRNA is an earlier and more rapid response than the translation from mRNA to proteins. An advantage of the proteomics approach is that it allows the finding of previously unknown molecules, in contrast to the cDNA microarray technology, which only regards known DNA sequences.

This study addresses the value of the functional genomics technologies using cDNA microarrays and two-dimensional gel electrophoresis-based proteomics in toxicology. For this evaluation, the well-studied toxicant bromobenzene (BB) was used to induce hepatotoxicity in rats. Bromobenzene is an industrial solvent that elicits toxicity predominantly in the liver, where it causes centrilobular necrosis. Like many xenobiotics, it is a hydrophobic molecule that is subjected to biotransformation in order to enable excretion in the urine. The metabolism and toxicity of bromobenzene in (rat) liver have been described in detail [9–14]. Bromobenzene is subjected to cytochrome P450-mediated epoxidation, followed by either conjugation with glutathione, enzymatic hydrolysis or further oxidation of the phenols, leading to hydroquinone-quinone redox cycling. At high BB doses, primarily due to conjugation to the epoxides or bromoquinones, hepatic cellular glutathione is depleted. This triggers a number of secondary reactions like lipid peroxidation, altered intracellular calcium levels, and mitochondrial dysfunction, ultimately leading to cell death. Housekeeping functions such as energy production, (protein) biosynthesis and cytoskeleton organisation might be disrupted. An important process in bromobenzene toxicity is the covalent binding of reactive BB metabolites to (specific) endogenous proteins, especially containing sulfhydryl groups [15]. Necrotic cells elicit responses from neighbouring cells like recruitment or induction of proteases. If the BB-induced damage does not lead to cell death, many genes and proteins involved in recovery and regeneration will be regulated to restore homeostasis. In the liver, the toxic effects are primarily observed at the centrilobular region, due to the high oxygen concentration and cytochrome P450 activity. After transport to the kidneys, bromobenzene induces nephrotoxicity mainly through BB-metabolites conjugated to glutathione that elicit oxidative stress.

A simple study design assesses the molecular toxicity of an intraperitoneal (i.p.) dose of bromobenzene, 24 hr after administration. cDNA microarray measurements were duplicated and two-dimensional gel electrophoresis were triplicated for each individual animal, while control groups of both untreated and vehicle treated rats were included. In-depth toxicological discussion of the results is beyond the scope of this evaluation of transcriptomics and proteomics in toxicology, and will be reported elsewhere [16]. Although toxicological interpretations are restricted by the limited design of the studies reported here, a comprehensive set of genes and proteins in rat liver is presented that change upon bromobenzene treatment and that may play a role in the mechanism of toxicity leading to hepatocellular necrosis. Using transcriptomics and proteomics techniques we were able to confirm previously reported effects and identify genes and proteins that were not recognised before in bromobenzene toxicity, involved in processes like drug metabolism, oxidative stress, reduced glutathione (GSH) depletion, the acute phase response and many more yet to be resolved.

2. Materials and methods

Unless otherwise indicated, all reagents were obtained from Sigma.

Bromobenzene 99% was from Sigma-Aldrich Chemie GmbH. Corn oil was from obtained from Remia.

2.1. Animal treatment

2.1.1. In vivo rat study

Male Wistar outbred rats (Charles River Deutschland), (10–12 weeks, bw: 225 ± 8 g) were injected i.p. with bromobenzene (5.0 mmol/kg bw, dissolved in corn oil, 40% v/v) or corn oil only, as vehicle control. Rats (3–4 per group) were treated with BB or with corn oil only, and an additional group contained the untreated controls. Rats had free access to food and drinking water and were treated according to Good Laboratory Practice (GLP) guidelines and protocols approved by the laboratory animal ethical committee. Rats were sacrificed by decapitation 24 hr after BB or corn oil (CO) administration. Livers were immediately dissected, quickly weighed, snap-frozen in liquid nitrogen, and stored at −80° until further processing. Livers were homogenised with a mortar and pestle in liquid nitrogen before preparing the total RNA and total protein extracts. Livers were isolated and processed in a random order to exclude biased results originating from sample preparation.

2.1.2. GSH determination

GSH + GSSG and oxidised glutathione (GSSG) levels in liver homogenate were determined using 5,5′dithiobis-2-nitrobenzoic acid (DTNB) to oxidise GSH and form 5-thio-2-nitrobenzoic acid (TNB) which was measured spectrophotometrically at 405 nm. GSSG was measured after derivatisation of GSH with 2-vinyl-pyridine [17].

2.1.3. Cytosolic glutathione-S-transferase activity

Microsomal and cytosolic fractions were isolated by ultracentrifugation from homogenised liver. The activity of glutathione-*S*-transferase in the cytosol of rat liver was determined using the model substrate CDNB (1-chloro-2,4-dinitrobenzene) according to [18]. Total protein concentration was determined according to the standard Bradford method using Biorad solution [19].

2.2. Transcriptomics

2.2.1. RNA extraction

Total RNA was extracted from liver homogenate using Trizol (Life Technologies S.A.) according to the manufacturer's protocol. Total RNA was further purified using the RNEasy RNA purification kit (Qiagen). RNA was checked for purity and stability by gel electrophoresis and the concentration was calculated from the extinction at 260 nm as determined spectrophotometrically.

2.2.2. Reference RNA

To allow comparison of all individual expression patterns, reference RNA was prepared. Dissected organs (liver (∼50% w/w of total), kidneys, lungs, brains, thymus, testes, spleen, heart, and muscle tissues) of several untreated male Wistar rats were flash-frozen in liquid nitrogen and stored at −80°. All tissues were homogenised together in liquid nitrogen before RNA isolation.

2.2.3. cDNA microarray preparation

About 3000 different sequence verified rat cDNA clones from the I.M.A.G.E. consortium were purchased (Research Genetics), and cDNA was amplified by PCR using forward (5′-CTGCAAGGCGATTAAGTTGGGTAAC-3′) and reverse (5′-GTGAGCGGATAACAATTTCACACAGGAAACAGC-3′) primers containing a 5′-C6-aminolinker (Isogen Bioscience) to facilitate crosslinking to the aldehyde coated glass microscope slides. PCR products were purified by ethanol precipitation and checked for purity and fragment size by electrophoresis on a 1% agarose gel. Purified PCR products were dissolved in 3× SSC and clones were arrayed in a controlled atmosphere on CSS-100 silylated aldehyde glass slides (TeleChem) (modified from DeRisi *et al.* [20]). In total, about 3800 cDNAs, including 3000 different rat genes, some in duplicate, and various control clones were deposited on the slides. After drying, slides were blocked with borohydride and stored in a dark and dust-free cabinet until further use. Prior to hybridisation, slides were prehybridised in buffer (5× SSC, 0.1% SDS, and BSA (10 mg/mL)) for 2 hr at 42°, washed in milliQ water, dipped in isopropanol and dried.

2.2.4. cDNA synthesis and labelling

A typical labelling reaction was performed using 50 μg of total RNA using an indirect procedure. *In vitro* transcription reactions were performed using reverse transcriptase according to the protocol with the Cyscribe Reagent Kit (Amersham Biosciences). In this reaction, amino allyl dUTP linkers were incorporated, after which the reaction mixture was divided over two portions for coupling with Cy3 or Cy5 fluorophores respectively. RNA was degraded by hydrolysis in NaOH (30 min at 37° and the mixture was neutralised with an equimolar amount of acetic acid. The cDNA was purified using the QIAquick spin columns (Qiagen) and water was evaporated. Pelleted cDNA was resuspended in 0.3 M sodium bicarbonate buffer, pH 9.0 and Cy3 or Cy5 fluorophores (freshly dissolved in DMSO) were chemically attached to the aminoallyl linkers. The reaction mixture was quenched with hydroxylamine (0.3 volumes, 4 M) for 1 min at room temperature to avoid non-specific fluorescence by free fluorophores. Labelled cDNA was purified from unincorporated fluorophores using an AutoseqG-50 (Amersham Biosciences) sephadex chromatography column. The amount of cDNA obtained and the incorporation rate of the fluorophore were determined spectrophotometrically. Prior to hybridisation, labelled cDNAs of both sample and reference were mixed and dissolved in 30 μL EasyHyb hybridisation buffer (Roche Diagnostics). Yeast tRNA (100 μg, Life Technologies S.A.)

and Poly dAdT (20 μg, Amersham Biosciences) were added to avoid non-specific binding. The hybridisation mixture was denatured for 1.5 min at 100° and pipetted onto a pre-hybridised microarray slide, covered with a plastic coverslip and, embedded in a slide incubation chamber (Corning, Life Sciences), submerged in a water bath for 16 hr at 42°. After hybridisation, slides were washed by firm shaking in 0.5× SSC buffer in a 50 mL tube and two times 10 min in 0.2× SSC on a mechanical shaking platform. Slides were dried quickly by centrifugation at 700 rpm.

2.2.5. Scanning

Slides were scanned immediately after drying using the ArrayWorxs CCD scanner (Applied Precision). The ArrayWorxs software processes the acquired images into results files, text files containing signal and local background intensity for both channels. Excel (Microsoft Corporation) was used to further process the data.

2.3. Transcriptomics experimental design

In order to compare many samples, individuals, or samples from different studies, an external reference was introduced. Each individual rat sample was co-hybridised with the reference RNA, prepared from untreated rat tissues. For each gene fragment, the amount of mRNA in the sample relative to the amount in the reference was determined. The complete set of hybridisations was duplicated with swapping of the two fluorophores incorporated in the sample and reference RNA. As a consequence of the introduction of the reference sample, comparisons are indirect, as the ratios 'treated/reference' and 'control/reference' are compared to obtain the desired 'treated/control' values. To assess whether different results are obtained using the indirect comparison, three direct co-hybridisations of one BB rat liver and one CO rat liver were performed and compared to the results obtained through indirect comparison of all the BB and CO samples relative to the reference.

2.3.1. Data analysis

For each spot, the local background intensity was subtracted from the signal intensity. Technical variations introduced during labelling of RNA samples with the two different fluorophores or by scanning have to be taken into account. It is assumed that the large part of the transcripts is equally present in both samples and the total fluorescence should be equal in both channels. Therefore, the sum of all background subtracted signals (if >0) of each channel was normalised to an arbitrary value of 1,000,000 to enable comparison between the channels but also between the microarrays. Background intensities outside the cDNA spots were very low and homogeneous. To account for non-specific hybridisation and background fluorescence of the cDNA on the slide, control spots were included on the microarrays containing cDNAs of fungal or yeast origin, with no significant homology to (known) rat cDNAs. Fluorescence intensity in these spots was used to determine a signal intensity threshold value. If background-corrected signal intensities were below a threshold value of 100 for any of the two channels, measurements were excluded from analysis. After doing so, one complete microarray, co-hybridised with RNA from BB-treated rat liver and reference RNA, was excluded from further analysis since too many spots did not meet the threshold value. Background-corrected and normalised signal intensities were used to calculate the ratio of gene expression of the sample over the reference. The group average fold change in gene expression relative to reference was calculated for the untreated, corn oil control, and bromobenzene groups (up to 8 values per group). Statistical significance of the difference in expression between these groups was analysed with a two-tailed Student's *t*-test for each gene, and differences were considered significant if the *P*-value did not exceed 0.01. The average fold changes of CO vs. UT and of BB vs. CO were calculated from the group average fold changes.

2.4. Proteomics

2.4.1. Sample preparation

Homogenised frozen liver was diluted 1:15 (w/v) with sample lysis buffer consisting of 8 M urea, 2% (v/v) CHAPS, 1% (w/v) DTT, 0.8% (v/v) Pharmalyte. Samples were further homogenised through a 25 in. gauge needle using a 10 mL syringe. Samples were centrifuged for 30 min at 100,000 *g* at 15°. Supernatant was stored in aliquots at −80° until further use. Protein was determined in homogenised liver using a dye-binding procedure [19] (Biorad).

2.4.2. Two dimensional gel electrophoresis, analytical gels

A total of 13 μL of homogenised liver sample (50 μg of protein) was overnight rehydrated in a volume of 350 μL in a Reswelling Tray on Immobiline DryStrip (IPG) pH 4–7 in 0.5% (v/v) CHAPS, 15 mM DTT, 0.5% (v/v) IPG buffer pH 4–7L. Isoelectric focusing of samples was performed on a Multiphor II Electrophoresis Unit for 45000 VH using the following program: 30 min at 150 V; 1 hr at 300 V; 1 hr at 1500 V and 12 hr and 20 min at 3500 V. Subsequently, IPG strips were equilibrated for 15 min in Equilibration buffer (6 M urea, 30% (w/v) glycerol, 2% SDS in 0.05 M Tris–HCl buffer, pH 8.8 containing 1% (w/v) tributylphosphine) and 0.001% (w/v) bromophenol blue. Next, IPG strips were equilibrated for 15 min in Equilibration Buffer containing 250 mM iodoacetamide. Second dimension electrophoresis was performed on custom made 12–15% polyacrylamide gels, using the Hoefer DALT Multiple Casting Chamber (Amersham Biosciences). Gels were prepared according to procedures recommended by the manufacturer. Gels were silver stained without glutaraldehyde, according to

the method described by Shevchenko *et al.* [21]. Scanning of gels was performed on a BioRad GS-710 Calibrated Imaging Densitometer (Bio-Rad).

2.4.3. Gel image and data analysis

Scanned TIFF images were analysed using Phoretix 2D Gel Analysis Software version 5.01 (Nonlinear Dynamics). For one of the bromobenzene treated rats, repeated attempts to obtain an analysable gel image were made, but the quality criteria were not met and no proteome data were analysed for this rat. For all other gels, spots were automatically detected and analysed images were scrutinised by eye for undetected or incorrectly detected spots. The total staining intensity within each detected spot, that is the amount of protein present, is defined as 'spot volume'. To compare spot volumes across different gels, the protein spots detected in each experimental gel were matched to the corresponding protein spots within a digitised reference spot pattern. Background intensity was subtracted from the spot volumes. To correct for differences in staining intensity between gels, spot volumes were divided by the volume of all spots and multiplied by the summarised total area of all spots. The resulting values represent the 'normalised spot volumes'. Differences in spot volumes from different treatment groups were analysed for statistical significance by two-tailed Student's *t*-tests (assuming normal distributions and equal variance) using Excel.

2.4.4. Two dimensional gel electrophoresis, preparative gels

Preparative gels for mass spectrometric identification of differentially expressed proteins spots were prepared similar to the analytical gels, except that at least 1 mg of protein was loaded per gel.

2.4.5. Mass spectrometry

For identification, protein spots were manually cut from the gel in a dust free cabinet to prevent contamination with keratin. Gel plugs were processed for mass spectrometry essentially according to Shevchenko *et al.* [21]. Silver stained gel pieces were destained with 30 mM potassium ferricyanide and 100 mM sodium thiosulphate (Merck), washed with water (MilliQ, Milllipore) and twice with acetonitrile (Biosolved B.V.). The liquid was substituted with reduction buffer (6.5 mM DTT in 50 mM NH_4HCO_3, pH 8.5) followed by a 60 min incubation at room temperature. The buffer was then replaced with acetonitrile which in turn was replaced with alkylation buffer (55 mM iodoacetamide in 50 mM NH_4HCO_3) and gel plugs were incubated for 30 min at room temperature in the dark. The gel pieces were dehydrated with acetonitrile and rehydrated with 50 mM NH_4HCO_3, pH 8.5 twice. Finally the gel pieces were dehydrated with acetonitrile and rehydrated in digestion buffer at 4° (50 mM NH_4HCO_3) containing 10 ng/μL trypsin, and then incubated overnight at 37°. Samples were centrifuged and the supernatant was transferred to micro ZipTip C18 pipette tips (Milllipore), and further processed according to the manufacturer's protocol. For MALDI-TOF-MS, the peptides were eluted directly from the ZipTip onto the MALDI target in 1–2 μL matrix solution (10 mg/mL α-cyano-4-hydroxycinnamic acid in 50% (v/v) acetonitrile, 0.1% trifluoroacetic acid). The peptide mixture for nano-electrospray MS/MS (NANO-ESI-MS/MS) was eluted from the ZipTip in 1–2 μL 50% (v/v) acetonitrile containing 0.1% (v/v) formic acid and transferred into a custom made nano-electrospray needle. The entire desalted digest from the silver stained spots was used for peptide mapping by MALDI-TOF-MS. When peptide extracts obtained from coomassie blue stained spots were used, the digest was split 1:4 for MALDI-TOF-MS peptide mapping and nano-electrospray MS/MS, respectively. MALDI-TOF-MS peptide mass spectra were recorded on an Applied Biosystems voyager DE-STR mass spectrometer in reflector and delayed extraction mode. The data were sampled with 4 GHz (0.5-ns channel width). All further processing including spectrum calibration based on the trypsin autodigest was performed using the software package DataExplorer 4.0 provided by the manufacturer. For further protein identification, a Micromass Q-tof mass spectrometer with a nanospray source was used for partial sequencing of the ZipTip desalted peptide mixture. A full scan was acquired over a wide mass range and precursor ions of interest were selected for MS/MS ion scan. This technique is well suited to high-sensitivity sequencing because there is no need for further chromatographic separation of the peptide mixture.

2.4.6. Database search mass spectrometry

Proteins were tentatively identified using the Mascot Search software (Matrix Science Ltd) to search the NCBInr (http://www.ncbi.nlm.nih.gov) protein database. The parameters were set to allow 1 miss cleavage with the enzyme trypsin and a peptide mass tolerance of 50–150 ppm. Additional protein information and calculation of theoretical pI and molecular mass were obtained from SwissPROT (http://www.expasy.ch).

2.4.7. Principal component analyses

To discern between transcriptome or protein profiles obtained from rats exposed to bromobenzene and controls, principal component analyses were performed. Principal component analysis (PCA) is a mathematical technique that reduces the many dimensions of a large dataset to a few dimensions that actually describe the large part of the variation in the samples without a priori knowledge. PCA was performed using EAGLES, an in house developed software package. The transcriptomics dataset consisted of all expression ratios of sample vs. reference of all genes left after quality filtering. Ratios were log transformed (base 10) for PCA analysis, and excluded values were replaced by a value of 0. A two-dimensional plot of the most

relevant principal components is used to visualise the difference in gene or protein expression profiles from the different rat livers, displayed as the objects in the plot. The larger the separation between two objects in the plot, the higher the degree of difference is between the expression profiles. All spot volumes from the three protein gels obtained from each animal were included in the analysis of the proteomics data. For each animal, triplicate scores (representing gels) are interconnected by lines resulting in triangles. By comparison of the distances between the centre of each triangles of different animals conclusions can be drawn with respect to the difference in proteomes.

3. Results

Rats received a single i.p. dose of bromobenzene and the effect on expression of proteins and genes in the liver was determined using proteomics and transcriptomics technologies. The bromobenzene dose was chosen based on previous studies to be hepatotoxic, and this was confirmed by the finding of a nearly complete glutathione depletion at 24 hr after bromobenzene administration (Fig. 1). Glutathione (GSH + GSSG) levels were lowered 27-fold from nearly 21 μmol/g liver in the corn oil controls to 0.8 μmol/g in the livers of bromobenzene treated animals. The low level of oxidised (GSSG) relative to reduced glutathione (GSH) indicates that the depletion is primarily due to conjugation and to a much lesser extent due to oxidation of glutathione. No changes in GSH levels were induced by corn oil administration. The bromobenzene administration resulted in on average 7% decrease in body weight after 24 hr, whereas vehicle control rats gained on average 6% of weight. The relative liver weights did not change significantly.

A significant average 1.4-fold increase ($P < 0.04$) in activity of glutathione-*S*-transferase towards CDNB was observed in the cytosolic liver fractions of rats treated with bromobenzene compared to vehicle controls, which showed activities similar to untreated controls.

3.1. Transcriptomics

Using cDNA microarrays, we determined the transcript levels of about 3000 different genes in rat liver, relative to the expression in a reference sample, in duplicated microarray hybridisation experiments for all rats individually. About 10–20% of the rat cDNA spots of each array contained no or very weak fluorescent signal, corresponding to genes that are not expressed or only below detection limits of the technology. After the quality filtering procedure as described in Section 2, the remaining elements were subjected to extensive analysis. The majority of the genes represented on our microarray was comparably expressed throughout all the samples. However, the bromobenzene treatment distinctly elicited alterations in the expression pattern of a number of genes in rat liver. The average fold changes in expression were calculated between BB treated vs. corn oil control (CO) rat livers, and between CO and untreated rat livers. Using the quality criteria described in Section 2, 32 genes were found to be significantly upregulated, and 17 were repressed more than 2-fold by bromobenzene treatment relative to the vehicle

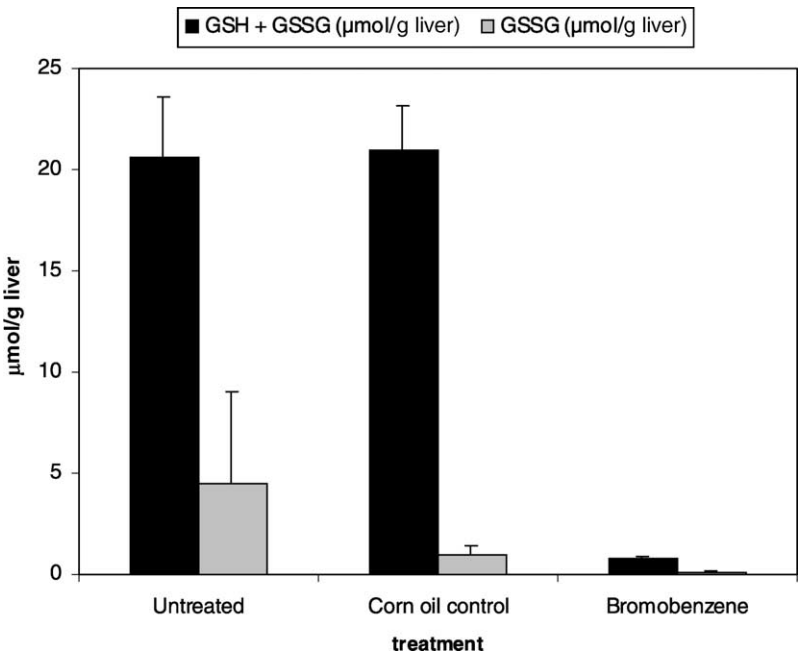

Fig. 1. Intracellular (GSH + GSSG) and (GSSG) levels. Intracellular (GSH + GSSG) and (GSSG) levels were determined of rat liver homogenate of untreated, corn oil controls and bromobenzene treated rats. An almost complete depletion of intracellular GSH levels occurred 24 hr after bromobenzene i.p. administration.

Table 1
Genes that changed expression significantly ($P < 0.01$) upon bromobenzene treatment were functionally grouped: drug metabolism

AC#	Gene name	Average CO/UT		Average BB/CO	
		Fold change	*P*-value	Fold change	*P*-value
AA900551	Epoxide hydrolase (microsomal EH)	0.76	0.340	5.59	0.000
AA923966	Aflatoxin B1 aldehyde reductase (AFAR)	1.04	0.766	4.70	0.000
AA955106	Aldehyde dehydrogenase (ALDH)	1.09	0.784	2.20	0.005
AA956507	NADPH-cytochrome P450 oxidoreductase	0.77	0.268	1.78	0.002
AA818917	Weakly similar to human NADH-ubiquinone dehydrogenase	0.79	0.193	1.54	0.010
AA818339	Glutathione-*S*-transferase Ya (GSTA)	0.84	0.101	3.70	0.000
AA998734	Glutathione-*S*-transferase, Mu type 2 (Yb2) (GSTM2)	0.97	0.923	2.58	0.004
AA818339[a]	Glutathione-*S*-transferase Ya (GSTA)	0.94	0.509	2.40	0.006
AA955668	Glutathione-*S*-transferase P subunit (GSTP)	1.00	0.953	1.39	0.006
AA819810	Weakly similar to rat glutathione-*S*-transferase P	1.32	0.063	0.46	0.001
AA819810[a]	Weakly similar to rat glutathione-*S*-transferase P	1.14	0.202	0.38	0.000

The table contains the GenBank accession numbers (AC#) of the cDNA fragments present on the microarray, the name of the gene, the average fold change in expression of both CO vs. UT and BB vs. CO, as well as the *P*-value of the Student's *t*-test. Average fold changes are listed ranked from increased to decreased.

[a] Duplicate cDNA fragment printed on the microarray.

Table 2
Genes that changed expression significantly ($P < 0.01$) upon bromobenzene treatment were functionally grouped: glutathione metabolism

AC#	Gene name	Average CO/UT		Average BB/CO	
		Fold change	*P*-value	Fold change	*P*-value
AA818339	Glutathione-*S*-transferase Ya (GSTA)	0.84	0.101	3.70	0.000
AA998734	Glutathione-*S*-transferase, mu type 2 (Yb2) (GSTM2)	0.97	0.923	2.58	0.004
AA965220	Gamma-glutamylcysteine synthetase light subunit (GCSl)	1.07	0.625	2.53	0.006
AA818339[a]	Glutathione-*S*-transferase Ya (GSTA)	0.94	0.509	2.40	0.006
AA955668	Glutathione-*S*-transferase P subunit (GSTP)	1.00	0.953	1.39	0.006
AA819810	Weakly similar to rat glutathione-*S*-transferase P	1.32	0.063	0.46	0.001
AA819810[a]	Weakly similar to rat glutathione-*S*-transferase P	1.14	0.202	0.38	0.000
AA964788	Glutathione peroxidase (GPX1)	1.10	0.554	0.37	0.001

The table contains the GenBank accession numbers (AC#) of the cDNA fragments present on the microarray, the name of the gene, the average fold change in expression of both CO vs. UT and BB vs. CO, as well as the *P*-value of the Student's *t*-test. Average fold changes are listed ranked from increased to decreased.

[a] Duplicate cDNA fragment printed on the microarray.

control, while respectively 63 and 35 genes were up- or downregulated when considering a more subtle (>1.5) fold change. Genes that changed expression significantly upon bromobenzene treatment were functionally grouped and listed in Table 1 (drug metabolism), Table 2 (glutathione), Table 3 (oxidative stress), Table 4 (acute phase response), Table 5 (protein synthesis), Table 6 (protein degradation), Table 7 (others, >1.5-fold change). Table 8 lists the genes that change significantly ($P < 0.01$) in rat liver after corn oil administration compared to untreated controls.

Table 3
Genes that changed expression significantly ($P < 0.01$) upon bromobenzene treatment were functionally grouped: oxidative stress

AC#	Gene name	Average CO/UT		Average BB/CO	
		Fold change	*P*-value	Fold change	*P*-value
AA874884	Heme oxygenase gene	0.99	0.976	5.20	0.001
AA817693	Ferritin light chain subunit	0.83	0.391	4.29	0.005
AA874884	Heme oxygenase (HO-1)	1.06	0.699	2.70	0.002
AA875245	Peroxiredoxin 1 (heme-binding protein 23)	0.96	0.805	2.61	0.000
AA875245[a]	Peroxiredoxin 1 (heme-binding protein 23)	0.92	0.413	2.04	0.001
AA818441	Ferritin-H subunit	0.89	0.415	2.01	0.004
AA957593	Tissue inhibitor of metalloproteinase-1 (TIMP1)	0.97	0.772	1.69	0.004

The table contains the GenBank accession numbers (AC#) of the cDNA fragments present on the microarray, the name of the gene, the average fold change in expression of both CO vs. UT and BB vs. CO, as well as the *P*-value of the Student's *t*-test. Average fold changes are listed ranked from increased to decreased.

[a] Duplicate cDNA fragment printed on the microarray.

Table 4
Genes that changed expression significantly ($P < 0.01$) upon bromobenzene treatment were functionally grouped: acute phase response

AC#	Gene name	Average CO/UT		Average BB/CO	
		Fold change	*P*-value	Fold change	*P*-value
AA817693	Ferritin light chain subunit	0.83	0.391	4.29	0.005
AA874884	Heme oxygenase (HO-1)	1.06	0.699	2.70	0.002
AA900218	Metallothionein-i (mt-1)	1.46	0.006	2.76	0.002
AA859399	Metallothionein	1.86	0.008	2.71	0.002
AA858741	Apolipoprotein M	1.21	0.253	2.05	0.001
AA818441	Ferritin-H subunit	0.89	0.415	2.01	0.004
AA819204	Weakly similar to rat Metallothionein-I	1.14	0.446	1.66	0.007
AA926277	CELF/C/EBP delta transcription factor	0.93	0.497	0.83	0.007
AA817963	Negative acute-phase protein alpha-1-inhibitor 3	0.62	0.007	0.64	0.008
AI072074	Fatty acid binding protein 1, liver	0.85	0.432	0.56	0.001
AA817963[a]	Negative acute-phase protein alpha-1-inhibitor 3	0.66	0.049	0.55	0.005
AA998796	Complement component C9 precursor	1.21	0.102	0.54	0.001
AA956238	Vitronectin	1.29	0.154	0.54	0.002
AA900592	Similar to human complement component Clr	1.23	0.136	0.53	0.000
AA901379	Inter-alpha-inhibitor H4P heavy chain	1.52	0.045	0.52	0.009
AA819267	Fibrinogen gamma chain-a	0.98	0.888	0.52	0.007
AI044677	Weakly similar to rat gamma-fibrinogen	1.84	0.010	0.51	0.004
AA963164	Synaptojanin II	1.00	0.987	0.49	0.004
AA819043	Fibronectin 1	0.88	0.389	0.47	0.000
AI137907	Alpha-1-macroglobulin	1.22	0.340	0.46	0.006
AA858975	Transferrin	0.92	0.616	0.46	0.006
AA819465	Apolipoprotein C-III	0.96	0.803	0.44	0.000
AI072074	Fatty acid binding protein 1, liver	1.09	0.687	0.42	0.006
AA963445	Selenoprotein P	1.10	0.619	0.39	0.002

The table contains the GenBank accession numbers (AC#) of the cDNA fragments present on the microarray, the name of the gene, the average fold change in expression of both CO vs. UT and BB vs. CO, as well as the *P*-value of the Student's *t*-test. Average fold changes are listed ranked from increased to decreased.

[a] Duplicate cDNA fragment printed on the microarray.

Table 1 lists the enzymes involved in drug metabolism that are responding upon BB treatment. Bromobenzene strongly induces the levels of mRNA encoding the liver glutathione-*S*-transferase Alpha and Mu subunits, the microsomal epoxide hydrolase (mEH) and the aflatoxin B1 aldehyde reductase (AFAR). Aldehyde dehydrogenase gene expression increased more than 2-fold upon bromobenzene treatment. Concurrently, the NADPH-cytochrome

Table 5
Genes that changed expression significantly ($P < 0.01$) upon bromobenzene treatment were functionally grouped: protein synthesis

AC#	Gene name	Average CO/UT		Average BB/CO	
		Fold change	*P*-value	Fold change	*P*-value
AI045792	Highly similar to rat 60S ribosomal protein L9	1.14	0.537	2.47	0.010
AA819544	Ribosomal protein S2	1.04	0.802	2.33	0.001
AA900657	60S ribosomal protein L7A	0.96	0.664	2.25	0.000
AA874997	Ribosomal protein S8	1.04	0.791	1.97	0.001
AA924912	Ribosomal protein L6	0.86	0.395	1.94	0.000
AA899448	Ribosomal protein S3a	0.78	0.448	1.89	0.006
AA818640	Highly similar to human 40S ribosomal protein S18	0.88	0.451	1.88	0.006
AA925200	60S ribosomal subunit protein L35	0.93	0.588	1.85	0.007
AA866268	Highly similar to RL8 human 60S ribosomal protein L8	1.10	0.391	1.71	0.002
AA818442	Ribosomal protein S11	0.89	0.174	1.70	0.001
AA900527	Ribosomal protein S26	0.92	0.451	1.52	0.009
AA924882	Ribosomal protein L15	0.98	0.798	1.41	0.005
AA998895	Nucleophosmin (nucleolar protein B23)	0.95	0.467	3.02	0.000
AA819244	Nuclear-encoded mitochondrial elongation factor G	0.51	0.051	2.31	0.004
AA874949	Similar to human initiation factor eIF-5A gene	0.88	0.448	1.95	0.001
AA875102	Highly similar to mouse/human small nuclear ribonucleoprotein E	0.85	0.263	1.62	0.001
AA964651	Highly similar to mouse prefoldin subunit 2	0.77	0.061	1.60	0.010
AA899472	Highly similar to rat eukaryotic translation initiation factor 3. Subunit 8	0.89	0.410	1.58	0.000

The table contains the GenBank accession numbers (AC#) of the cDNA fragments present on the microarray, the name of the gene, the average fold change in expression of both CO vs. UT and BB vs. CO, as well as the *P*-value of the Student's *t*-test. Average fold changes are listed ranked from increased to decreased.

Table 6
Genes that changed expression significantly ($P < 0.01$) upon bromobenzene treatment were functionally grouped: protein degradation[a]

AC#	Gene name	Average CO/UT		Average BB/CO	
		Fold change	*P*-value	Fold change	*P*-value
AA859498	Cathepsin L	0.83	0.395	3.53	0.037
NA	Cathepsin L	0.94	0.622	3.21	0.007
AA859484	Proteasome (prosome. Macropain) subunit beta type 3	0.96	0.654	2.27	0.000
AA859300	Proteasome (prosome. Macropain) subunit alpha type 1	1.00	0.994	1.73	0.014
AI030596	Similar to human 26S proteasome subunit S5B	1.15	0.412	1.60	0.054
AA859582	Proteasome subunit beta type 5 precursor (epsilon chain)	1.30	0.229	1.57	0.057
AI043800	ESTs, highly similar to 26S proteasome-associated pad1 homologue; 26S proteasome non-ATPase subunit (human and mouse)	0.86	0.672	1.47	0.043
AA964414	Proteasome component C8	0.92	0.507	1.40	0.089
AA925795	Proteasomal ATPase (SUG1)	0.96	0.659	1.30	0.054

The table contains the GenBank accession numbers (AC#) of the cDNA fragments present on the microarray, the name of the gene, the average fold change in expression of both CO vs. UT and BB vs. CO, as well as the *P*-value of the Student's *t*-test. Average fold changes are listed ranked from increased to decreased.
[a] All induced proteasome and cathepsin genes are listed. *P*-values indicate significance of the induction).

P450 oxidoreductase was significantly upregulated. In contrast to the glutathione-*S*-transferase (GST) Alpha, Mu and Pi subunits' upregulation, the 'EST weakly similar to (rat) GST Pi subunit' decreased over 2-fold. Sequence analysis of this cDNA fragment (AC# AA819810) revealed similarity to the rat GST class Pi 7-7 (gi:121749) at the amino acid sequence level. Genes involved in the metabolism of intracellular glutathione that changed upon BB treatment are listed in Table 2. Besides the induction of glutathione-*S*-transferases, a 2.5-fold upregulation of γ-glutamylcysteine synthetase (γ-GCS), the key enzyme in GSH biosynthesis was observed. GSH peroxidase, an enzyme also implicated in oxidative stress was found to be downregulated. Genes typically responding to oxidative stress such as heme oxygenase-1, peroxiredoxin 1 (heme binding protein 23), metallothioneins, ferritin, TIMP1 were found to be induced (Table 3).

Bromobenzene treatment elicits changes in transcript levels of many of the so-called acute phase proteins. Ferritin, apolipoprotein M and metallothionein are induced in the acute phase response (APR) and were found to be strongly induced by the BB treatment. Moreover, negative APPs including alpha-1-inhibitor 3, alpha-1-macroglobulin, transferrin, complement components, liver fatty acid binding protein 1 and fibrinogen are downregulated 24 hr after bromobenzene treatment (Table 4).

Interestingly, many ribosomal subunits and other factors involved in protein synthesis (Initiation factor, elongation factor) were induced upon BB treatment (Table 5). Furthermore, Table 6 lists the induction of several components of the proteasome and of the proteolytic enzyme cathepsin L from the lysosome. Many genes with interesting implications in other cellular processes (Table 7) were found to be upregulated such as beta actin, glucose-6-phosphate dehydrogenase, thyrotropin receptor, cytochrome *c*, cytochrome b5, cysteine sulfinic acid decarboxylase and clathrin. Genes downregulated by BB include a mitochondrial ATPase inhibitor, thymosin beta 10, betaine homocysteine methyl transferase (BHMT), cysteine dioxygenase, hemoglobin, insulin-like growth factor and mitochondrial HMG-CoA synthase.

Only a few liver transcripts markedly changed in expression caused by corn oil injection (Table 8). Metallothionein, the ''EST weakly similar to (rat) fibrinogen gamma'', and C4 complement protein were significantly upregulated by CO. These are proteins modulated in the acute phase response and interestingly, the latter two were downregulated by BB (Table 4). The negative acute phase protein alpha-1-inhibitor was significantly downregulated in the CO controls, and levels decreased further in the BB treated rats. The mRNA for cytochrome P450 oxygenase 2E1 (CYP2E1) was downregulated on average 1.6-fold by corn oil.

Principal component analysis (PCA) was applied to visualise the differences in the expression profiles from treated and non-treated rats (Fig. 2). The expression profiles of rat liver after BB treatment are clearly distinct from the controls. In the plot, the horizontal distance (PC#1) between the groups of BB treated and control liver expression profiles is larger than the distance between samples within one group. The injection of corn oil only as the vehicle control did not result in aberrant gene expression profiles compared to the untreated samples. The vertical distance (PC#2) between samples in the plot does not reflect relevant biological effects but technical variation. The distance between two expression profiles obtained from the same rat indicates that the technical variation introduced by the RNA labelling and hybridisation procedures provides the main source of variation within a treatment group. The interindividual biological variation within the treatment groups did not exceed the technical variation. Additionally, the principal component values were calculated per gene and genes were ranked according to the PC#1 values. The genes with the largest PC#1 values are differentially expressed after treatment. Genes with positive PC#1 values proved to be upregulated by bromobenzene, whereas genes with negative values were downregulated by BB compared to controls. The genes that

Table 7
Genes that changed expression significantly ($P < 0.01$) upon bromobenzene treatment were functionally grouped: other functions

AC#	Gene name	Average CO/UT		Average BB/CO	
		Fold change	*P*-value	Fold change	*P*-value
AI059976	Vesl-2	0.94	0.739	3.77	0.001
AA964496	Highly similar to actin beta	1.14	0.585	3.48	0.005
AA858998	RAN. Member RAS oncogene family	0.91	0.740	2.88	0.004
AI030685	Nestin	0.98	0.917	2.44	0.007
AI060085	Thyrotropin receptor	1.10	0.426	2.36	0.002
AA964725	Highly similar to mouse Flightless I homolog Drosophila	1.18	0.615	2.35	0.008
AA965078	Mitochondrial 3,2-*trans*-enoyl-CoA isomerase	1.01	0.876	2.22	0.006
AI045953	Cysteine sulfinic acid decarboxylase	1.02	0.949	2.17	0.004
AI059951	Neuronal cell death related gene in neuron-7 (DN-7)	1.10	0.124	2.01	0.001
AA818887	MHC class I	0.92	0.509	1.96	0.004
AA956323	Membrane bound cytochrome b5	0.78	0.225	1.90	0.000
AI058620	Bax inhibitor-1 (BI-1) (testis enhanced gene transcript)	1.09	0.627	1.89	0.002
AI058566	Peptide/histidine transporter	1.06	0.669	1.82	0.001
AA874955	Clathrin light chain (LCB3)	0.78	0.063	1.80	0.001
AA900595	Anti-silencing protein ASF1 homolog	1.10	0.241	1.80	0.000
AA964548	Highly similar to rat tubulin beta chain	0.99	0.949	1.79	0.000
AA866442	Somatic cytochrome *c*	0.64	0.227	1.77	0.006
AA900102	Mitochondrial import inner membrane translocase subunit TIM8 A	1.00	0.982	1.74	0.005
AA899102	Glucose-6-phosphate dehydrogenase	0.98	0.861	1.73	0.003
AA874837	Phosphoglycerate mutase B isozyme (PGAM)	0.82	0.195	1.73	0.007
AA819314	Initiation factor 2 associated 67 kDa protein; methionine aminopeptidase	0.78	0.129	1.72	0.010
AA859476	Cofilin	0.81	0.166	1.69	0.006
AI453996	Heat shock 70 kDa protein 5; Glucose regulated protein	0.96	0.720	1.68	0.004
AA964657	EST unknown	0.96	0.744	1.64	0.005
AA964651	Highly similar to mouse prefoldin subunit 2	0.77	0.061	1.60	0.010
AA875070	Alpha-prothymosin	0.94	0.659	1.58	0.006
AI043642	Potassium channel (KCNQ2)	1.00	0.978	1.53	0.003
AA957012	Highly similar to human RNA polymerase II chain	1.00	0.980	0.68	0.001
AA866264	Weakly similar to rat 20-alpha-hydroxysteroid dehydrogenase	0.92	0.524	0.66	0.010
AI070597	Highly similar to human CGI-97 protein	1.60	0.002	0.65	0.009
AA925346	Cytochrome P450 51, lanosterol 14-alpha-demethylase	1.10	0.257	0.61	0.000
AA818579	Cysteine dioxygenase	0.76	0.175	0.58	0.009
AA963258	Insulin-like growth factor I (IGF-I)	1.12	0.528	0.55	0.009
AA819034	Alpha interferon inducible protein	1.31	0.155	0.54	0.008
AI136048	Mitochondrial 3-hydroxy-3-methylglutaryl-CoA synthase	1.45	0.094	0.53	0.008
AA819784	Hemoglobin. Alpha 1	1.39	0.165	0.52	0.010
AA926010	Long-chain acyl-CoA synthetase	1.12	0.543	0.46	0.002
AA901407	Betaine homocysteine methyltransferase (BHMT)	0.67	0.057	0.45	0.003
AA924288	Thymosin beta-10 gene	0.77	0.399	0.42	0.005
AA858662	Tryptophan 5-monooxygenase activation protein (Ywhaz)	0.82	0.175	0.41	0.000
AA819164	Mitochondrial IF1 ATPase inhibitor	0.96	0.848	0.41	0.005
AA926359	Receptor-linked protein tyrosine phosphatase (PTP-PS)	1.18	0.305	0.39	0.000

The table contains the GenBank accession numbers (AC#) of the cDNA fragments present on the microarray, the name of the gene, the average fold change in expression of both CO vs. UT and BB vs. CO, as well as the *P*-value of the Student's *t*-test. Average fold changes are listed ranked from increased to decreased.

Table 8
Genes that change significantly ($P < 0.01$) more than 1.5-fold by corn oil injection compared to untreated controls

AC#	Gene name	Average CO/UT		Average BB/CO	
		Fold change	*P*-value	Fold change	*P*-value
AA964554	Highly similar to human U3 snoRNP-associated 55-kDa protein	2.54	0.009	0.59	0.164
AA859399	Metallothionein	1.86	0.008	2.71	0.002
AI044677	Weakly similar to rat gamma-fibrinogen	1.84	0.010	0.51	0.004
AI070597	Highly similar to human CGI-97	1.60	0.002	0.65	0.009
AA900218	Metallothionein-i (mt-1)	1.46	0.006	2.76	0.002
AA957923	Mast cell protease II gene	0.68	0.001	1.25	0.108
AA818896	Cytochrome P450j (CYP2E1)	0.63	0.010	1.39	0.128
AA817963	Negative acute-phase protein alpha-1-inhibitor 3	0.62	0.007	0.64	0.008

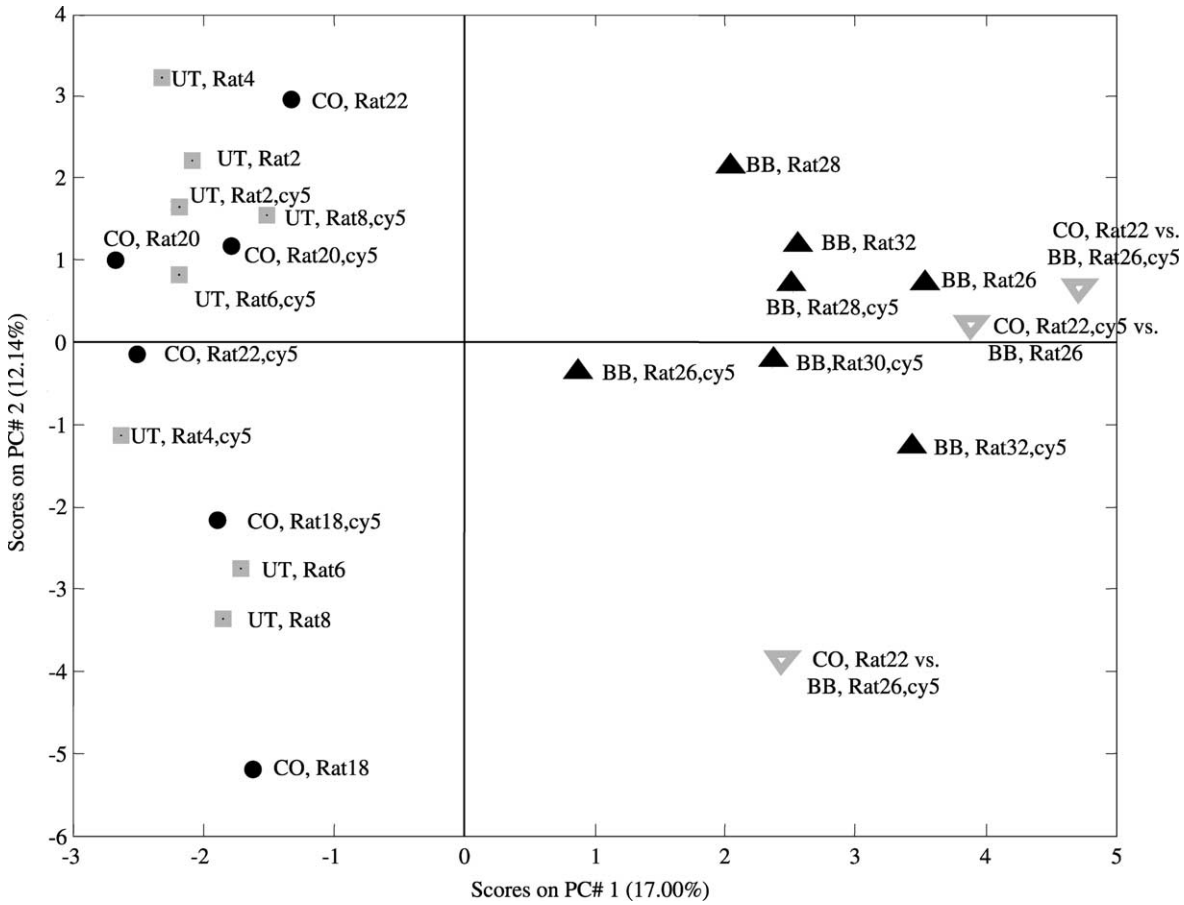

Fig. 2. Principal component analysis of transcriptome data. Objects in the plot represent expression profiles from individual rat livers. The two principal components explaining the majority of the variation in the dataset are plotted. Clearly, the expression profiles of rat liver after BB treatment are distinct from the controls. The injection of corn oil only as the vehicle control did not result in aberrant gene expression profiles compared to the untreated samples. UT: untreated (squares); CO: corn oil vehicle control (circles); BB: bromobenzene treated (triangles); directly compared BB vs. CO samples (inverted triangles). Individual rat numbers are indicated, followed by 'Cy5' when the liver RNA sample was labelled with Cy5 fluorophore (and the reference with Cy3). In the other samples, the fluorophore incorporation was swapped.

account for most of the differences in the expression profiles of BB-treated compared to controls in the PC-analysis were found to be the identical genes that were identified by fold-change calculations (Tables 1–7).

PC-analysis indicated a cluster of genes which most pronouncedly contributed to bromobenzene induced hepatotoxicity. This cluster contained several drug metabolising enzymes like the microsomal epoxide hydrolase 1 (mEH), glutathione-*S*-transferase Alpha (GSTA), Mu (GSTM) and Pi subunits and aflatoxin B1 aldehyde reductase (AFAR). Moreover, proteins related to oxidative stress response like ferritin (both heavy and light subunit), heme oxygenase-1 (HO-1), peroxiredoxin 1 and NADPH cytochrome P450 oxidoreductase were elevated in concordance. Most of the genes considerably downregulated were identified as acute phase proteins.

To test whether similar results are obtained using direct or indirect hybridisations including a general reference sample, three co-hybridisations of one BB rat liver and one CO rat liver mRNA sample were performed and compared to the results obtained through indirect comparison of all the BB and CO samples. Relative expression levels should correlate well for all genes, but especially the differential expression of genes should be identified similarly using both approaches. Therefore, the BB/CO fold change of 165 genes identified in the indirect approach to be differentially expressed with >1.5-fold change (*t*-test $P < 0.02$) was compared to the average fold change as measured in three replicated BB vs. CO co-hybridisations, resulting in a correlation coefficient of 0.879.

3.2. Proteomics

At least 3 two-dimensional gels were prepared from each liver extract. A reference protein pattern was constructed from rat liver, containing 1124 protein spots. In Fig. 3, the protein pattern obtained from an untreated animal is shown. Spot numbers and identities—whenever available—of 24 proteins that were differentially expressed in bromobenzene or corn oil treated animals are indicated. Fig. 4 displays the volumes for all spots identified as statistically significantly changed upon bromobenzene or corn oil treatment. The

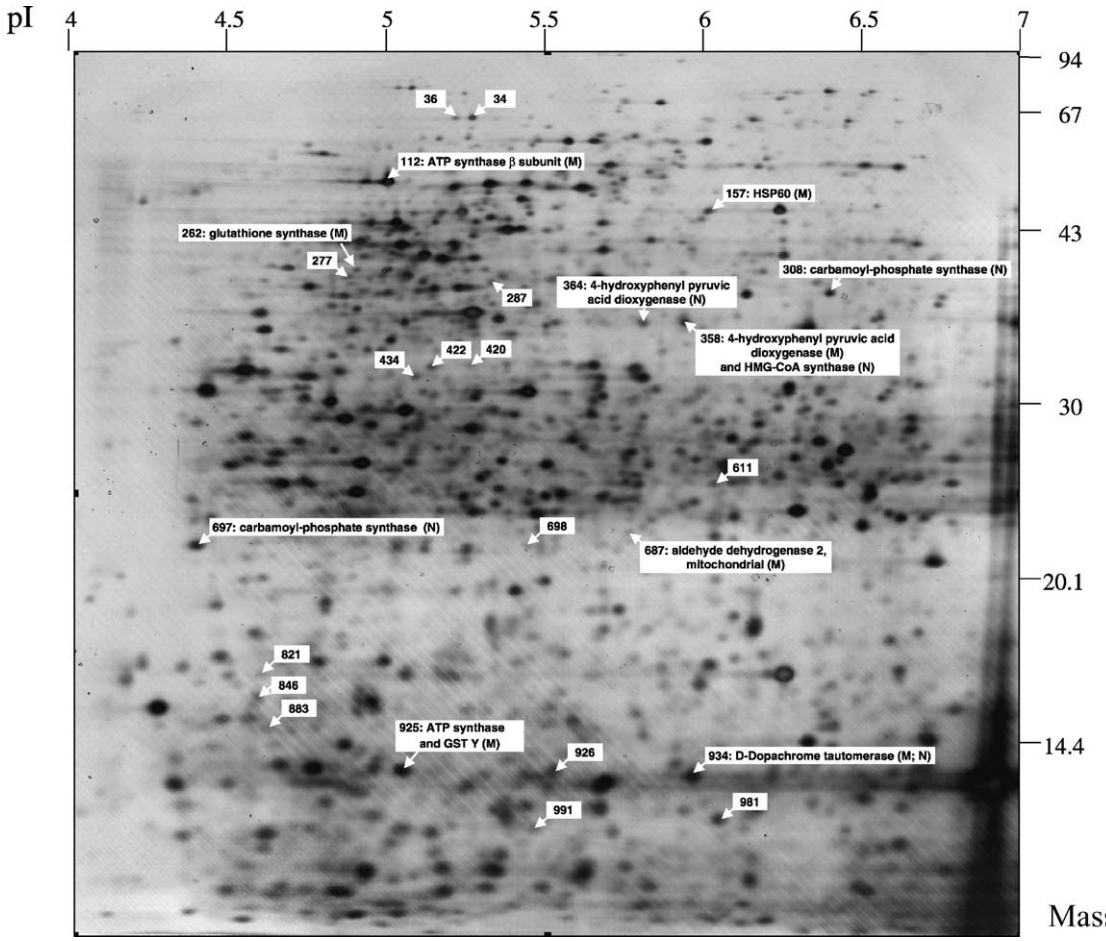

Fig. 3. Two-dimensional gel electrophoresis of liver from untreated rat. A two-dimensional gel electrophoresis obtained from an untreated animal is shown. Spot numbers and identities—whenever available—of proteins that were differentially expressed in bromobenzene-treated animals are indicated. The method of identification is indicated: M: MALDI-TOF-MS; N: ESI-MS/MS.

bars represent normalised spot volumes, averaged for all (9–12) gels within one treatment group (untreated, vehicle control or bromobenzene treated). Hence, the depicted standard deviation reflects both the interanimal variation, as well as technical variation between gels.

Part of the spots marked as significantly changing were identified by MALDI-TOF or nano-electrospray mass spectrometry. Spot 112 was identified as the ATP synthase beta subunit (gi:1374715). The level of ATP synthase beta subunit decreased ~3.5-fold upon bromobenzene treatment. Peptide fragments from spot 925, which also decreased by bromobenzene were found to match the mitochondrial ATP synthase alpha subunit (liver isoform) (gi:114523). Remarkably, other peptide fragments isolated from this same spot matched the glutathione-*S*-transferase Y subunit (gi:204503). The peptide fragment pattern obtained from protein spot 157 was found to match a protein sequence from the murine Heath Shock Protein 60 (gi:51452). Sequence alignment (BLAST at NCBI) indicated that the amino acid sequence is more than 99% identical to the *Rattus norvegicus* HSP60 (gi:1334284). The expression of HSP60 decreased about 3-fold upon bromobenzene treatment as compared to control groups. Peptide fragments from both spot 358 and spot 364 were identified as 4-hydroxyphenylpyruvic acid dioxygenase (HPD, gi:8393557), using MALDI-TOF-MS and ESI-MS-MS, respectively. HPD converts 4-hydroxyphenylpyruvate dioxygenase to homogentisate and is involved in tyrosine catabolism. HPD decreased ~5.5-fold upon treatment with bromobenzene, part of which could be explained by an effect of corn oil. Both spots represent proteins with similar molecular mass, however, a slight difference in pI was found. Repeated peptide fragment analyses, using ESI-MS-MS, of spot 358 isolated from two new gels revealed a mixture of fragments that matched HPD and peptide fragments that matched hydroxymethylglutaryl-CoA synthase (HMG-CoA synthase, gi:123330). Spot 687 was identified as mitochondrial aldehyde dehydrogenase 2 (gi:14192933). Aldehyde dehydrogenase 2 increased ~2.5-fold upon bromobenzene exposure, whereas i.p. administration of corn oil did not induce changes in the protein content. Peptide fragments derived from spot 934 matched with fragments from the D-dopachrome tautomerase gene (DOPA, gi:13162287). DOPA is an enzyme catalysing the tautomerisation of D-dopachrome to 5,6-dihydroxyindole. D-dopachrome tautomerase decreased upon corn oil treatment, but not

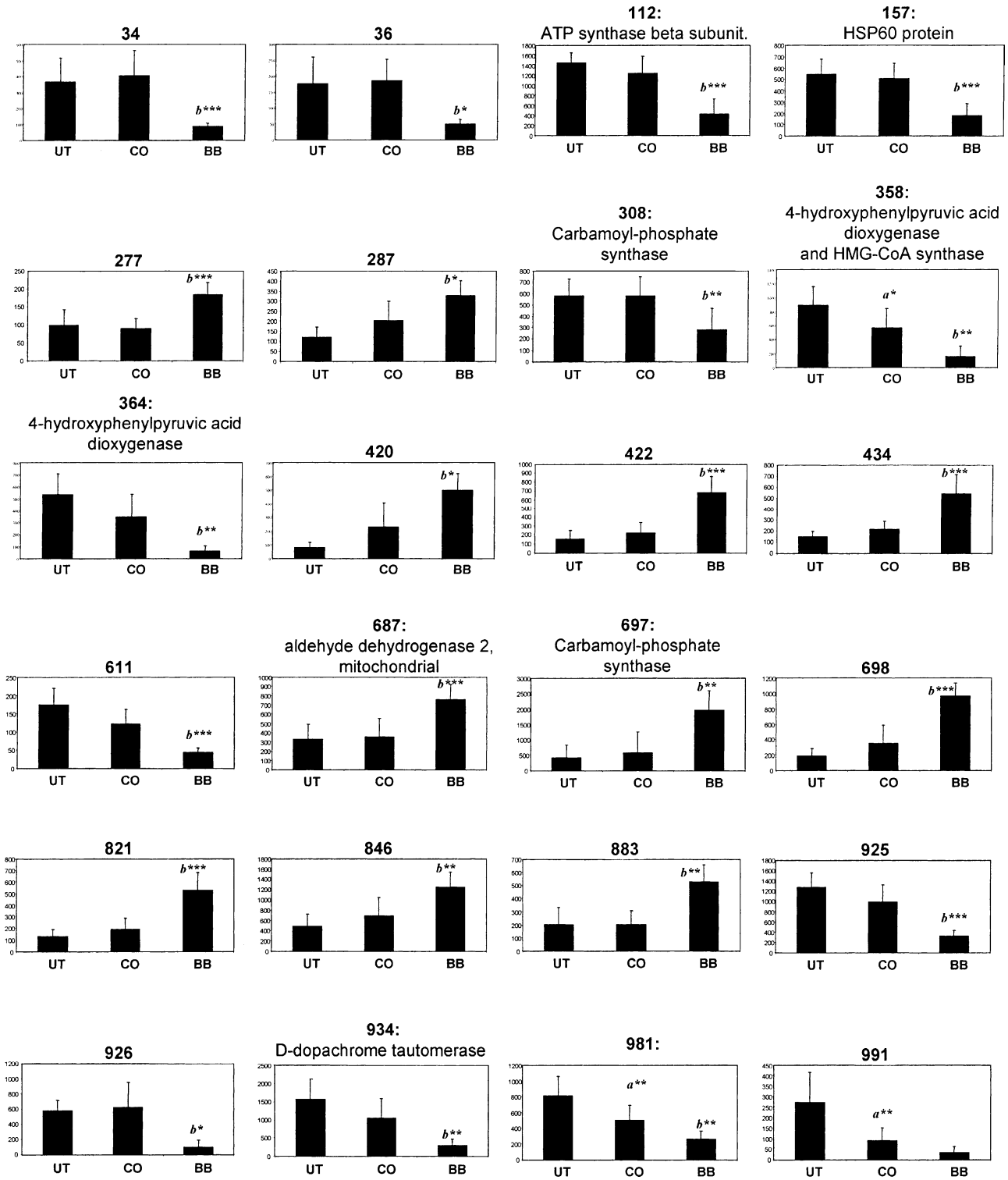

Fig. 4. Protein spots that changed statistically significant upon corn oil (CO), or bromobenzene (BB) treatment. Average spot volume + SD obtained from all gels within a group is shown. UT: untreated; CO: corn oil vehicle control; BB: bromobenzene. (a) Significant difference (two-tailed Student's *t*-test) between untreated and corn oil vehicle control treated animals. (b) Significant difference (two-tailed Student's *t*-test) between bromobenzene and corn oil treated animals. $^{*}P < 0.05$; $^{**}P < 0.005$; $^{***}P < 0.001$. Protein names of identified spots are indicated.

statistically significant. However, a significant further decrease in expression level was caused by bromobenzene treatment. Spots 308 and 697 both were identified as carbamoyl-phosphate synthase (CPSI, gi:117492), an enzyme involved in the urea cycle (E.C. 6.3.4.16). Spot 308, corresponding with a high molecular mass protein (~40 kDa), decreases upon BB treatment, whereas spot 697 corresponds with a smaller (~25 kDa) protein which

amount increases upon BB. Spot 262 was found to be induced by BB 1.5-fold compared to corn oil and 2-fold compared to UT, but no statistical significance could be shown due to one outlier intensity value in the CO group, resulting in standard deviation of over 50% for the CO group (not shown). Mass spectrometry identified peptide fragments of this spot matching to glutathione synthetase (gi:1170038), an enzyme involved in the GSH synthesis.

Besides the few proteins found to statistically significantly change with corn oil and bromobenzene treatment, a decrease in the average size of the proteins in the bromobenzene livers as compared to the corn oil livers is observed in Fig. 5. In all gels from BB-treated livers, less spots are present in the upper (large mass proteins) region of the gels and more spots appear in the lower region compared to both CO and UT controls. Principal component analysis on the proteomics data (Fig. 6) also illustrates a clear difference between liver protein patterns of bromobenzene-treated animals and controls. Each object in the plot represents all normalised spot volumes from one

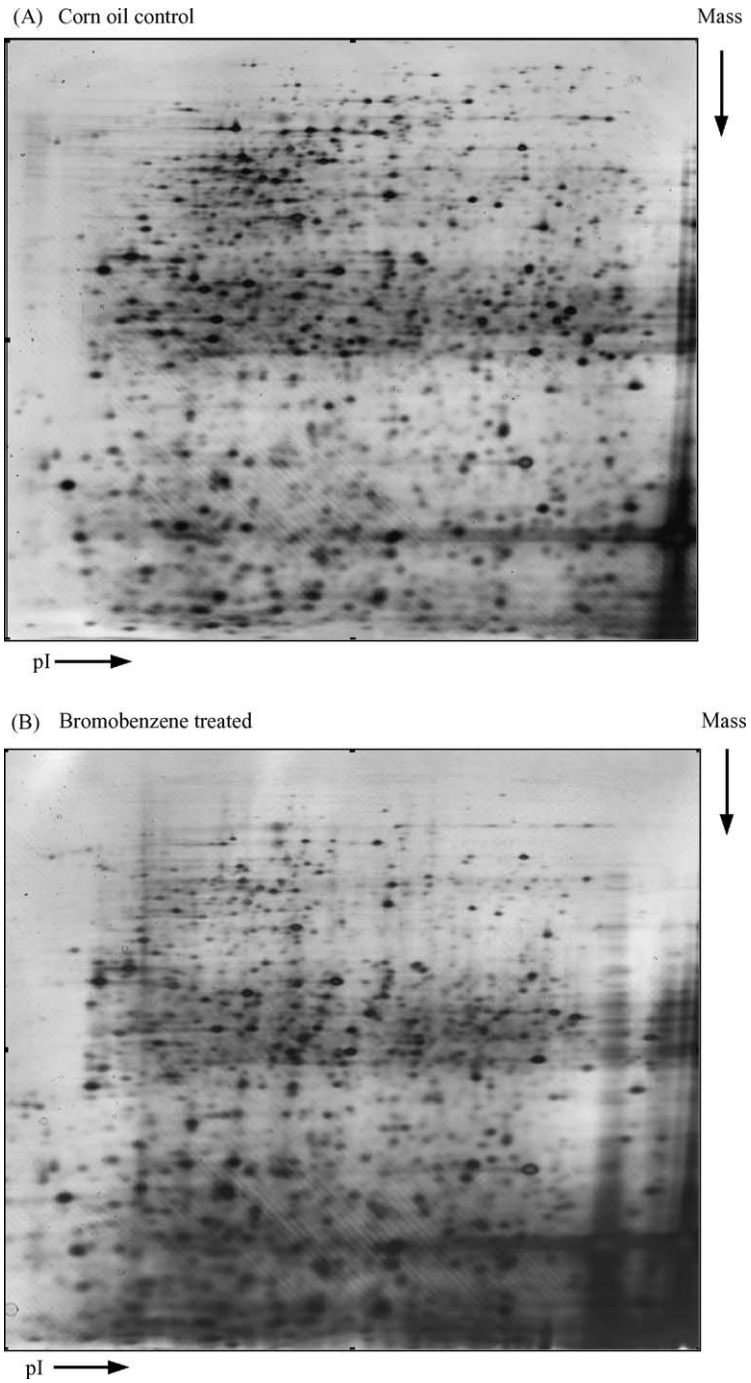

Fig. 5. Representative gel images from liver of control and bromobenzene-treated rats. (A) Corn oil treated vehicle control; (B) Bromobenzene treated. These images show a shift towards proteins with lower molecular mass after bromobenzene treatment.

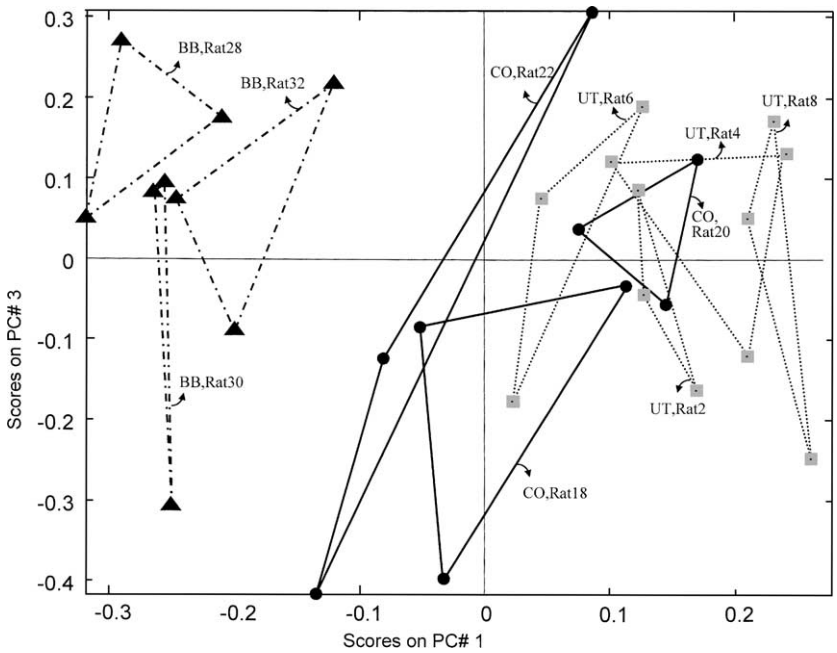

Fig. 6. Principal component analysis of proteomes. PCA was applied using spot volume data obtained from untreated, corn oil control and bromobenzene-treated animals. The two principal components explaining the majority of the variation in the dataset are plotted. Individual gels of bromobenzene treatment samples are displayed by triangles, circles indicate the corn oil controls and squares the untreated samples. The three gels from the same animal are connected by lines. Protein patterns from bromobenzene treated animals are clearly distinct from corn oil and untreated controls. A slight difference in the pattern of corn oil treated animals as compared to untreated rats could be concluded from this image.

gel. There is a relatively large distance between objects of the BB treatment group to the objects of both control groups. The distance between the three objects from the same rat is generally larger than distance between samples from different animals, indicating that technical variations exceed the interindividual variations within treatments groups.

4. Discussion

Novel functional genomics technologies are applied to toxicology to aid the study of cellular mechanisms of toxicity. The combined application of transcriptomics and proteomics methods was evaluated in a toxicological experiment in rats with a typical hepatotoxicant, bromobenzene. Acute toxicity by i.p. bromobenzene administration is known to lead to centrilobular necrosis in the liver. In elaborate studies of the effects on rat liver gene expression with multiple doses of bromobenzene and time points of analysis, we determined expression profiles that correspond well with the results presented here; a comparable oral dose (5 mmol/kg bw) of bromobenzene elicited distinct responses at 24 hr, while 6 hr after dosage, responses were not yet pronounced. Administration of lower doses of bromobenzene induced fewer changes in the transcriptome. Changes at the expression level are related to other toxicity parameters [16].

The observed glutathione depletion and body weight decrease 24 hr after dosage are physiological symptoms that concur with many changes at the mRNA and protein level in the liver, presented in this report. The depletion of cellular GSH content can not be explained by the formation of GSSG from oxidation of two GSH molecules, since the GSSG content does not increase. Rather, GSH depletion reflects the exhaustive use of GSH in conjugation to reactive BB metabolites catalysed by GSTs, or through spontaneously conjugation. The strong induction of GST Alpha, Mu and Pi subunit mRNAs that was found (Table 1) corroborates the importance of GSH conjugation by these enzymes in the biotransformation of bromobenzene. The significant 1.4-fold increase in cytosolic GST activity towards CDNB, 24 hr after BB dosage, confirms the functional implications of the observed induction of GST isozymes at the mRNA level. Catalysis of CDNB turnover is effected by several cytosolic GST isozymes, while GST Alpha is the most abundant enzyme in rat liver and presumably responsible for the large part of activity towards CDNB. The pivotal role of the depletion of intracellular GSH levels in the process of bromobenzene toxicity was strengthened by the finding of the induced gene expression of γ-glutamylcysteine synthetase, which is the rate-limiting enzyme in GSH synthesis. Induction has been reported under conditions where cellular GSH was depleted, and provides the cell with the ability to reconstitute GSH levels. The other enzyme important in the GSH synthesis, GSH synthase, was not found to change significantly at the mRNA level. However, at the protein level, a bromobenzene-induced increase in GSH synthase (spot 262) was found although one outlier value in the control

prevented statistical corroboration of this change. Additionally, the downregulation of GSH peroxidase is probably directly related to GSH depletion and has been shown in acetaminophen toxicity as well [23]. Thus, both transcriptomics and proteomics results provide complementary information to the changes in biochemically determined cellular GSH levels and specific enzyme activity of GST in the cytosol.

The induction of mRNA for microsomal epoxide hydrolase is coherent with its role in bromobenzene metabolism; the hydrolysis of the toxic epoxide BB intermediates. Microsomal epoxide hydrolase is expressed strongly in liver, but also found in many other organs. It is induced by xenobiotics like phenobarbital, *trans*-stilbene oxide and Aroclor 1254 [24]. Expression of the cytosolic epoxide hydrolase gene was not significantly changed upon bromobenzene treatment. The co-ordinate response of a cluster of genes upregulated by BB consisting of genes like GSTA, GSTM, γ-GCS, HO-1 and ferritin, peroxiredoxin1 and NADPH-cytochrome P450 oxidoreductase might reflect a common regulatory mechanism. Indeed, many of the genes in this cluster have been shown to be under transcriptional control of the Electrophile Response Element (EpRE, formerly named antioxidant response element, ARE). [25,26]. We speculate that more genes in this cluster could be under transcriptional control of the EpRE, probably activated by the BB epoxide metabolites, which are very strong electrophilic species. Heme oxygenase upregulation is a characteristic response to hepatic oxidative stress. Hypoxia, endotoxins, and xenobiotics that induce oxidative stress (e.g. cadmium chloride [27], acetaminophen [23]) were all found to induce heme oxygenase. The upregulation of hepatic heme oxygenase 1 by bromobenzene has been described long ago [28]. HO-1 is the enzyme that catalyses the degradation of heme into biliverdin, and induction could be functional against oxidative stress [29]. Bilirubin, produced from biliverdin by biliverdin reductase is an antioxidant, which would provide the cell with a defence mechanism against reactive oxygen species. The co-induction of HO-1 and peroxiredoxin1 was described before after exposure to heme or heavy metals $CdCl_2$ and $CoCl_2$ [22].

The i.p. administration of a high dose of bromobenzene clearly elicits a response well-known as the APR, as can be concluded from the differential expression of the genes listed in Table 4. The APR is a response of the organism to various types of stress like mechanical damage (liver regeneration after partial hepatectomy), systemic inflammation (endotoxins like lipopolysaccharides) or local inflammation [30,31]. Especially in the liver, the APR coincides with dramatic changes in a wide variety of proteins with the general purpose to provide a protective response and re-establish cellular homeostasis. A major function of the liver, the production of secreted proteins like plasma proteins, is heavily disturbed. The so-called negative acute phase proteins are downregulated in the APR, and comprise plasma transport proteins like albumin, hemopexin, ceruloplasmin and alpha1-acid glycoprotein. The expression of genes that encode for proteins with protective effects, for instance sequestering of reactive oxygen species, is upregulated in APR. Proteins like ferritin, metallothioneins, and alpha-fetoprotein are regarded as positive acute phase proteins. The injection of corn oil as a control elicits the downregulation of the alpha-1-inhibitor and the upregulation of one metallothionein species. Remarkably, fibrinogen is upregulated by corn oil, in contrast to the downregulation by BB.

The expression of 260 genes in liver and kidney of mice exposed to bromobenzene has been measured and compared to treatment with various chemicals by Bartosiewicz *et al.* [32]. A very high dose of BB (2.5 g/kg bw) was given, causing all mice to die within 48 hr post-dosage. Indeed, the approximate lethal dose in mice was reported to be 0.9 g/kg [33].The authors compared BB toxicity to CCl_4-induced toxicity and reported 15 genes to be regulated 24 hr after administration, both in BB as well as in CCl_4-treated mice, including strong upregulation of hsp25, c-*jun*, gadd45, γ-GCS and downregulation of CYP2E. Also, some genes were found to be regulated by BB but not by CCl_4, including GST Yc, CYP2B9, myeloid differentiation and P450 reductase. Several genes were identified to change in concordance with our findings, (e.g. γ-GCS and glutathione-*S*-transferases), however, patterns of gene expression also showed marked differences. Bartosiewicz *et al.* found more genes related to general stress pathways to be induced, possibly because a very high dose of bromobenzene was given. Moreover, mice were used whereas rats were studied in our work, which could account for species-specific differences in response.

A correlation was found for the gene and protein expression changes in aldehyde dehydrogenase. At the protein level, bromobenzene induced a 2.5-fold increase in the mitochondrial aldehyde dehydrogenase 2. Using cDNA microarrays, significant (over 2-fold) changes in the expression level of aldehyde dehydrogenase and also of aflatoxin B1 aldehyde reductase were found. The induction of aldehyde dehydrogenase and reductase may be an adaptation both at the gene and protein level to increased levels of 4-hydroxy-2-nonenal that could result from bromobenzene induced lipid peroxidation [34,35].

The 3.5-fold decrease in ATPase beta subunit protein concentration upon bromobenzene treatment probably indicates mitochondrial toxicity and a loss of cellular energy production in line with mitochondrial damage. Previous studies indicated the ability of bromobenzene to deplete ATP-levels *in vitro* and *in vivo* [36,37]. The protein decrease could not be related to changes in mRNA levels, as the cDNA microarray measurements for the ATPase subunits were inconclusive. Along with the ATPase decrease, the gene expression of the mitochondrial IF1 ATPase inhibitor was strongly inhibited. Recently, it was shown that acetaminophen-induced hepatotoxicity also

resulted in decreased ATP-synthase subunit and HSP60 levels in mice [8].

Upon BB treatment, the amount of Heat Shock Protein 60 (HSP60), 4-hydroxyphenylpyruvic acid dioxygenase (HPD) and D-dopachrome tautomerase (DOPA) decreased. Remarkably, two spots represent HPD protein with similar molecular mass but different pI, suggesting that HPD exists in more than one state, possibly through post-translational protein modification. ESI-MS-MS analyses of spot 358 cut from two new gels revealed both fragments that matched HPD as well as peptide fragments that matched hydroxymethylglutaryl-CoA synthase. The decrease in intensity of this spot can not be directly related to decreased expression of either HPD or HMG-CoA synthase as both might contribute to the decrease. Downregulation of HPD was concluded from analysis of protein spot 364, whereas 1.9-fold downregulated gene expression was found for HMG-CoA synthase. DOPA is catalysing the tautomerisation of D-dopachrome to 5,6-dihydroxyindole, which is a melanin precursor. DOPA is related to macrophage migration inhibitory factor (MIF) both by sequence and by enzyme activity. Moreover, MIF acts as a phenylpyruvate tautomerase, and is expressed at sites of inflammation, with a suggested role in regulating macrophages in host defence. Whether the change in DOPA levels has any toxicological implications related to MIF functions is unclear. A putative toxicological explanation for the observed decrease in HSP60 and HPD has yet to be determined. The decrease in the carbamoyl-phosphate synthase (CPSI) of ~40 kDa and the concordant increase in the smaller (~25 kDa) protein upon BB treatment propose a degrading activity towards this protein and provide an example of the capability to visualise protein processing with two-dimensional gel electrophoresis.

No statistically significant changes were observed in the gene expression levels of DOPA and HPD (clones AA924020 and AA900788, respectively, on the cDNA microarray) upon bromobenzene treatment. Unfortunately, cDNAs representing HSP60 and CPSI were not present on the microarray.

Proteomics data indicated that bromobenzene induced a shift in the protein pattern from high molecular mass proteins towards more lower molecular mass species (Fig. 5), which could indicate bromobenzene-induced degradation of proteins. All samples were processed randomly and the shift was only observed in the treated samples. The mRNA level for the lysosomal proteolytic enzyme cathepsin L significantly increased 3.5-fold upon BB injection, and many subunits of the proteasome complex were also found to be induced, although statistical probabilities were lower (Table 6). The bromobenzene-specific degradation of proteins through induced proteasome and cathepsin L activity might provide an explanation for the protein pattern shift observed in the gels. Besides, bromobenzene metabolites are known to covalently interact with protein sulfhydryl groups [15]. This protein adduction may target proteins for ubiquitinylation, resulting in activation of an ATP/ubiquitin-dependent proteolytic pathway mediated by the proteasome complex. Induced transcription of many factors involved in protein synthesis such as ribosomal proteins, translation initiation and elongation factors, could be an indication of increased protein synthesis (Table 5). Together with increased degradation, a higher protein turnover rate is suggested. Alternatively, the mechanism of protein synthesis could be affected in bromobenzene toxicity resulting in premature termination of protein translation explaining the shift in observed protein mass. Further investigations are required to identify the presence of incomplete proteins.

The fact that only 24 proteins were found to significantly change in all animals upon bromobenzene treatment seems to contradict the massive shift in the proteome pattern observed in the gel images (Fig. 3). The application of strict quality criteria provides the main explanation for the limited identification of significantly changing spots. The low number of proteins that were found to significantly change using the proteomics approach, is also in contrast to the many genes that were found to be differentially expressed. This is partly explained by known non-linearity between mRNA synthesis and protein concentration and the temporal difference in responses. Moreover, technical limitations of the two-dimensional gel electrophoresis in terms of protein abundance, solubility and physico-chemical properties apparently prevented the detection of many proteins for which corresponding mRNA level changes were observed using transcriptomics. For about half of the proteins that were found to significantly change, the identification by mass spectrometry was not successful, either because we could not recover protein from the preparative gels or because an interpretable mass spectrum was not obtained. Indications for post-translational protein modifications were obtained from the detection of two forms of 4-hydroxyphenylpyruvic acid dioxygenase with similar mass but slightly different pI, and the carbamoyl phosphate synthase that was identified twice with differing pI and molecular mass.

The results presented here acknowledge the possibilities to study toxicology at the molecular level using transcriptomics and proteomics technologies. The confirmation of previously identified effects as well as the finding of genes and proteins not yet known to be involved in BB-induced liver toxicity indicates that these technologies have the capability to expand insights in toxicology. Secondly, this evaluation stresses the difficulties and limitations in combining transcriptomics and proteomics results. While functional genomics technologies result in thousands of gene and protein measurements, many results can not be established with high confidence. Therefore, these methods require the application of strict quality filtering procedures, which we believe are of crucial importance for the outcome of the experiments. Due to the strict quality criteria, only a few proteins were identified as changing upon bromobenzene

treatment, frustrating the finding of matching results from transcriptomics and proteomics analyses. Especially the proteomics technique using mass spectrometry-based protein identification after two-dimensional gel electrophoresis does not easily allow the large scale identification of proteins involved in BB toxicity. However, new high throughput proteomics technologies (e.g. protein arrays) are being developed at high speed. While transcriptomics methods rapidly provide broad insights in cellular mechanisms, the determination of actual cellular protein and metabolite levels is required for the detailed elucidation of cellular processes in toxicity.

Acknowledgments

The authors thank Dr. Ted van der Lende, Evelyn Wesseling, Mieke Havekes, Annemiek Andel and Dr. Frank Schuren for excellent expertise and setting up of the microarray facility. Michèle van den Wijngaard and Anja Luiten for assistance in sample isolation. Mirjam Damen (Department of Biomolecular Mass Spectrometry, Utrecht University) for protein mass spectrometry analysis, and Pol Adriaansen for his help in analysing the gel electrophoresis data.

References

[1] Burczynski ME, McMillian M, Ciervo J, Li L, Parker JB, Dunn RT, Hicken S, Farr S, Johnson MD. Toxicogenomics-based discrimination of toxic mechanism in HepG2 human hepatoma cells. Toxicol Sci 2000;58:399–415.

[2] Bulera SJ, Eddy SM, Ferguson E, Jatkoe TA, Reindel JF, Bleavins MR, De La Iglesia FA. RNA expression in the early characterization of hepatotoxicants in Wistar rats by high-density DNA microarrays. Hepatology 2001;33:1239–58.

[3] Waring JF, Jolly RA, Ciurlionis R, Lum PY, Praestgaard JT, Morfitt DC, Buratto B, Roberts C, Schadt E, Ulrich RG. Clustering of hepatotoxins based on mechanism of toxicity using gene expression profiles. Toxicol Appl Pharmacol 2001;175:28–42.

[4] Waring JF, Ciurlionis R, Jolly RA, Heindel M, Ulrich RG. Microarray analysis of hepatotoxins in vitro reveals a correlation between gene expression profiles and mechanisms of toxicity. Toxicol Lett 2001; 120:359–68.

[5] Hamadeh HK, Bushel PR, Jayadev S, Martin K, DiSorbo O, Sieber S, Bennett L, Tennant R, Stoll R, Barrett JC, Blanchard K, Paules RS, Afshari CA. Gene expression analysis reveals chemical-specific profiles. Toxicol Sci 2002;67:219–31.

[6] Yoshida K, Kobayashi K, Miwa Y, Kang CM, Matsunaga M, Yamaguchi H, Tojo S, Yamamoto M, Nishi R, Ogasawara N, Nakayama T, Fujita Y. Combined transcriptome and proteome analysis as a powerful approach to study genes under glucose repression in *Bacillus subtilis*. Nucleic Acids Res 2001;29:683–92.

[7] Eymann C, Homuth G, Scharf C, Hecker M. *Bacillus subtilis* functional genomics: global characterization of the stringent response by proteome and transcriptome analysis. J Bacteriol 2002;184:2500–20.

[8] Ruepp SU, Tonge RP, Shaw J, Wallis N, Pognan F. Genomics and proteomics analysis of acetaminophen toxicity in mouse liver. Toxicol Sci 2002;65:135–50.

[9] Thor H, Svensson SA, Hartzell P, Orrenius S. Biotransformation of bromobenzene to reactive metabolites by isolated hepatocytes. Adv Exp Med Biol 1981;136(Pt A):287–99.

[10] Casini AF, Pompella A, Comporti M. Liver glutathione depletion induced by bromobenzene, iodobenzene, and diethylmaleate poisoning and its relation to lipid peroxidation and necrosis. Am J Pathol 1985;118:225–37.

[11] Monks TJ, Hinson JA, Gillette JR. Bromobenzene and *p*-bromophenol toxicity and covalent binding in vivo. Life Sci 1982;30:841–8.

[12] Lau SS, Monks TJ. The contribution of bromobenzene to our current understanding of chemically-induced toxicities. Life Sci 1988;42: 1259–69.

[13] Miller NE, Thomas D, Billings RE. Bromobenzene metabolism in vivo and in vitro. The mechanism of 4-bromocatechol formation. Drug Metab Dispos 1990;18:304–8.

[14] den Besten C, Brouwer A, Rietjens IM, van Bladeren PJ. Biotransformation and toxicity of halogenated benzenes. Hum Exp Toxicol 1994;13:866–75.

[15] Koen YM, Williams TD, Hanzlik RP. Identification of three protein targets for reactive metabolites of bromobenzene in rat liver cytosol. Chem Res Toxicol 2000;13:1326–35.

[16] Heijne WHM, *et al.* Toxicogenomics of bromobenzene-induced hepatotoxicity. 2003; in preparation.

[17] Anderson ME. Determination of glutathione and glutathione disulfide in biological samples. Methods Enzymol 1985;113:548–55.

[18] Habig WH, Pabst MJ, Jakoby WB. Glutathione-*S*-transferases. The first enzymatic step in mercapturic acid formation. J Biol Chem 1974; 249:7130–9.

[19] Bradford MM. A rapid and sensitive method for the quantitation of microgram quantities of protein utilizing the principle of protein–dye binding. Anal Biochem 1976;72:248–54.

[20] DeRisi JL, Iyer VR, Brown PO. Exploring the metabolic and genetic control of gene expression on a genomic scale. Science 1997;278: 680–6.

[21] Shevchenko A, Jensen ON, Podtelejnikov AV, Sagliocco F, Wilm M, Vorm O, Mortensen P, Shevchenko A, Boucherie H, Mann M. Linking genome and proteome by mass spectrometry: large-scale identification of yeast proteins from two dimensional gels. Proc Natl Acad Sci USA 1996;93:14440–5.

[22] Immenschuh S, Iwahara S, Satoh H, Nell C, Katz N, Muller-Eberhard U. Expression of the mRNA of heme-binding protein 23 is coordinated with that of heme oxygenase-1 by heme and heavy metals in primary rat hepatocytes and hepatoma cells. Biochemistry 1995;34:13407–11.

[23] Noriega GO, Ossola JO, Tomaro ML, Batlle AM. Effect of acetaminophen on heme metabolism in rat liver. Int J Biochem Cell Biol 2000;32:983–91.

[24] Oesh F, Arand M. Xenobiotic metabolism. In: Toxicology. London, UK: Academic Press; 1999. p. 83–110.

[25] Friling RS, Bensimon A, Tichauer Y, Daniel V. Xenobiotic-inducible expression of murine glutathione-*S*-transferase Ya subunit gene is controlled by an electrophile-responsive element. Proc Natl Acad Sci USA 1990;87:6258–62.

[26] Tsuji Y, Ayaki H, Whitman SP, Morrow CS, Torti SV, Torti FM. Coordinate transcriptional and translational regulation of ferritin in response to oxidative stress. Mol Cell Biol 2000;20:5818–27.

[27] Alam J, Wicks C, Stewart D, Gong P, Touchard C, Otterbein S, Choi AM, Burow ME, Tou J. Mechanism of heme oxygenase-1 gene activation by cadmium in MCF-7 mammary epithelial cells. Role of p38 kinase and Nrf2 transcription factor. J Biol Chem 2000;275: 27694–702.

[28] Guzelian PS, Elshourbagy NA. Induction of hepatic heme oxygenase activity by bromobenzene. Arch Biochem Biophys 1979;196:178–85.

[29] Hill-Kapturczak N, Chang SH, Agarwal A. Heme oxygenase and the kidney. DNA Cell Biol 2002;21:307–21.

[30] Ramadori G, Christ B. Cytokines and the hepatic acute-phase response. Semin Liver Dis 1999;19:141–55.

[31] Suffredini AF, Fantuzzi G, Badolato R, Oppenheim JJ, O'Grady NP. New insights into the biology of the acute phase response. J Clin Immunol 1999;19:203–14.
[32] Bartosiewicz M, Penn S, Buckpitt A. Applications of gene arrays in environmental toxicology: fingerprints of gene regulation associated with cadmium chloride, benzo(a)pyrene, and trichloroethylene. Environ Health Perspect 2001;109:71–4.
[33] Szymanska JA. Hepatotoxicity of brominated benzenes: relationship between chemical structure and hepatotoxic effects in acute intoxication of mice. Arch Toxicol 1998;72:97–103.
[34] Benedetti A, Pompella A, Fulceri R, Romani A, Comporti M. Detection of 4-hydroxynonenal and other lipid peroxidation products in the liver of bromobenzene-poisoned mice. Biochim Biophys Acta 1986; 876:658–66.
[35] Benedetti A, Pompella A, Fulceri R, Romani A, Comporti M. 4-Hydroxynonenal and other aldehydes produced in the liver in vivo after bromobenzene intoxication. Toxicol Pathol 1986;14:457–61.
[36] Locke SJ, Brauer M. The response of the rat liver in situ to bromobenzene—in vivo proton magnetic resonance imaging and ^{31}P magnetic resonance spectroscopy studies. Toxicol Appl Pharmacol 1991; 110:416–28.
[37] Wang BH, Zuzel KA, Rahman K, Billington D. Protective effects of aged garlic extract against bromobenzene toxicity to precision cut rat liver slices. Toxicology 1998;126:213–22.